photonics

MDPI

Communication

Application of the Improved Grinding Technology to Freeform Surface Manufacturing

Lirong Peng [1,2], Xingchang Li [2], Lingzhong Li [2], Qiang Cheng [2,*], Xiao Luo [2], Xiaoqin Zhou [1] and Xuejun Zhang [2]

[1] School of Mechanical and Aerospace Engineering, Jilin University, Changchun 130025, China
[2] Changchun Institute of Optics, Fine Mechanics and Physics, Chinese Academy of Sciences, Changchun 130033, China
* Correspondence: chengq@ciomp.ac.cn

Abstract: In order to meet the manufacturing requirements of modern space remote sensors for high-precision freeform optical parts, the grinding technology and its application were studied. The objective of this paper was to improve the application effect of traditional grinding technology in the processing of hard and brittle materials, and then apply it in specific fields. Therefore, the influence of key process factors such as cutting speed and removal depth on subsurface damage (SSD) was studied based on orthogonal experiments, and an improved grinding technology characterized by low SSD and high surface shape accuracy was formed. Then, the effect of this grinding technology was further verified by the high-precision manufacturing of freeform surfaces. A surface of a 130 mm diameter freeform surface was machined by improved grinding technology and combined polishing technology, the final root mean square of surface shape reached 12.1 nm. The improved grinding technology can reduce SSD from 20 μm to 10 μm, and improve the manufacturing efficiency of freeform surfaces above 30% when the cut speed is 20 m/s and the remove depth is 10 μm. The proposed technology can be applied to the extreme manufacturing of hard and brittle materials.

Keywords: optical manufacturing; ultra-precision grinding; freeform surface; bonnet polishing

Citation: Peng, L.; Li, X.; Li, L.; Cheng, Q.; Luo, X.; Zhou, X.; Zhang, X. Application of the Improved Grinding Technology to Freeform Surface Manufacturing. *Photonics* **2023**, *10*, 240. https://doi.org/10.3390/photonics10030240

Received: 5 February 2023
Revised: 19 February 2023
Accepted: 20 February 2023
Published: 22 February 2023

1. Introduction

Freeform surfaces can significantly improve the imaging quality and reduce the size and quality of the optical system [1]. It has been widely applied in aerospace, astronomical observation, high-tech civil, and other fields [2]. Meanwhile, the optical remote sensor has gradually developed into the prospect of high-technology, complexity, and multi-function [3]. The demand for a high-precision freeform surface has become more and more urgent, and higher requirements are proposed for its accuracy, geometric parameters, quality, and roughness [4].

In recent years, with the rapid development of space optical remote sensing technology, the applied optical frequency band of imaging optics is from far infrared to extreme ultraviolet. Its applications include earth observation fields such as the agricultural monitoring, and resource survey, intelligent transportation, and national security, as well as the space observation fields such as solar fine spectral observation and extra solar systems [5]. With the improvement of spatial resolution, spectral resolution, and temporal resolution of space remote sensors, higher requirements were put forward for the extreme manufacturing of optical parts. Optical parts are developing to the extreme manufacturing directions of ultra lightweight, ultra smooth surface, ultra-high precision, and ultra-low surface damage; this posed more severe challenges to traditional processing methods [6].

Wide applications of freeform surfaces also necessitate higher requirements for their design and manufacture. The machining of freeform surfaces is a complex process, which is divided into grinding, pre-polishing, and precision polishing [7]. Grinding is the first step of the optical process, the forming accuracy, surface roughness, and subsurface damage

directly determine the whole manufacturing cycle and final accuracy of the optical parts. Several models based on various parameters were used to predict the depth of subsurface damage (SSD), but most of these conclusions were semi-empirical and pay little attention to process improvement [8,9]. Usually, the subsurface damage depth of a fused quartz material grinded by traditional fixed abrasive was about 15–20 μm. Meanwhile, serious mid-frequency error on the ground surface greatly affects the subsequent polishing efficiency and manufacturing accuracy [10,11]. For this reason, some researchers try to reduce the SSD depth to less than 10 μm by using loose abrasive grind, but the efficiency was low, and the surface shape accuracy was often more than 10 μm [12]. Hence, it is necessary to optimize the key process parameters to reduce the depth of SSD in the fixed abrasive grinding process and improve the manufacturing efficiency and quality.

In this study, a generally applicable improved grinding technology was developed and applied to the manufacture of free-form surfaces. Therefore, this study designed orthogonal experiments of cutting speed and removal depth, and measured the SSD depth under different process conditions through sample experiments. By the above experiments, we obtained the improved grinding technology characterized by high surface accuracy and low SSD. Then, we try to apply it to the field of freeform surface machining to complete the engineering verification of the process. The improved grinding technology will provide important reference for the processing of other materials, and accelerated development of optical fabrication processes for new optical design.

2. Materials and Methods

2.1. Experiment Design

The grinding of hard and brittle materials was a process of material removal by repeated scratching of multiple abrasive particles under the condition of coolant supply [13]. This paper combined the actual working conditions and considered the state distribution of most abrasive particles in the process of fixed multi-abrasive grinding to design an orthogonal experiment. In this study, fused quartz plane with a diameter of 40 mm was selected as an experimental material. Grinding was performed on a Satisloh G1-2P (Satisloh, Wilhelm, Germany) by using a hemispherical tool (100 mm radius of curvature), of which the diamond size was 18 μm. In this case, the influence of removal depth and cutting speed on SSD was explored.

Several key factors should be taken into consideration in the design of the removal depth experiment. Firstly, the initial surface error of the experimental element after grinding was almost within the range of 2–3 μm, so the minimum removal depth was set to 5 μm to ensure the processing could traverse all positions of the element. Secondly, the surface shape error of the element will increase in actual processing considering the increase in element diameter, tool wear, and mechanical motion accuracy, and the removal depth should increase accordingly. Thirdly, the maximum removal depth of 30 μm can not only cover most surface error, but also reach an acceptable precision grinding load level. Based on the above principles, the influence of removal depth on surface damage was explored when the cutting speed was 20 m/s. The experimental design is shown in Table 1.

Table 1. Influence of removal depth and cut speed on SSD.

Number	a	b	c	d
Removal depth (μm)	5	10	20	30
Cut speed (m/s)	12	18	24	30

The experimental design of cutting speed mainly took into account the following factors. The empirical value range of traditional ultra-precision grinding cutting speed was 16–28 m/s, but for specific machining objects, the optimal value range needed to be investigated. In addition, the cutting speed was related to the spindle speed, and excessive speed will lead to a significant vibration. Consider the speed limit of tool spindle, the best

cut speed was generally between 1/3–2/3 of the spindle limit speed. On the basis of the above factors, the influence of cutting speed on surface damage was explored when the removal depth was 10 μm. The experimental design was shown in Table 1.

2.2. SSD Measurement and Analysis

Magneto rheological finishing (MRF) is considered as a near nondestructive polishing method [9]. In this experiment, MRF will be used to expose SSD layer by layer. Firstly, sample parts were grinded according to the above design. After grinding, each sample part was polished by MRF (CIOMP, HAAS VF5-M, Changchun, China), a removal function one-dimensional linear wedge was created ranging in depth from 5 to 20 μm on the sample part surface. Furthermore, the polished area of each sample part was characterized by optical microscopy to view the exposed SSD cracks at various polished depths along the MRF wedge. The position of the detection area was located by scanning the two-dimensional contour curve of the remove function through profilometer, and then the depth information corresponding to the detection feature was determined. Figure 1 illustrates the process schematically.

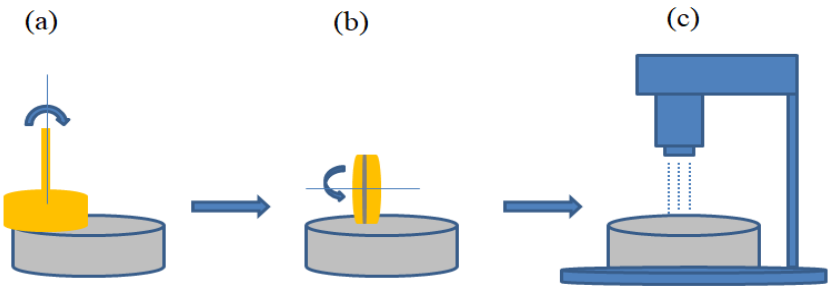

Figure 1. Schematic illustration of measured SSD characteristics, (**a**) Grinding, (**b**) MRF, (**c**) Microscope.

The schematic diagram of the analysis process was shown in Figure 2. Figure 2a shows the sample part after being ground and polished with a wedge. Figure 2b shows the surface shape of the taper; this was detected by profilometer and the points to be measured were marked at the different removal depths. In the experiment, optical microscopy was used to observe the damage characteristics along the slope at an interval of 1 mm. After removing the material of 1 μm depth, Figure 2c shows that obvious damage can be observed on the surface. When the material removal depth was increased to 2.5 μm, the damage characteristics were reduced significantly, as show in Figure 2d. Figure 2e illustrates that there was no subsurface damage existing in this material layer when the remove depth is 6 μm.

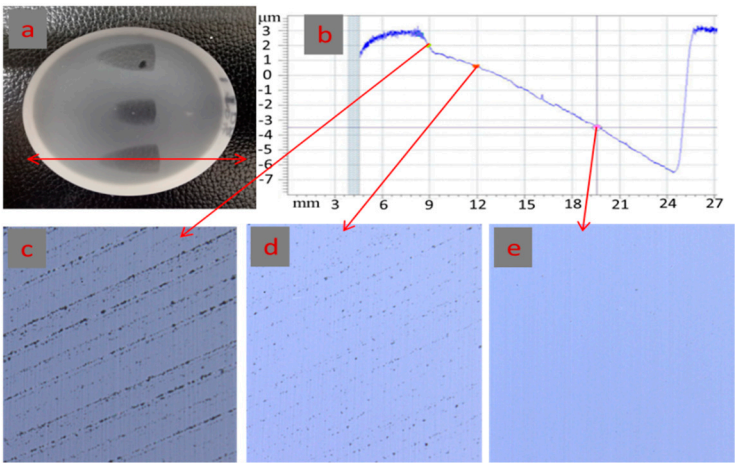

Figure 2. The schematic diagram of the analysis process, (**a**) sample part after being ground and polished with a taper; (**b**) two dimensional morphology of the taper; (**c**–**e**) Microscopic morphology after the removal depth increasing from 1 μm, 3 μm to 6 μm.

2.3. Experimental Verification on Freeform

Due to the geometrical complexity and high precision requirements of freeform surfaces for various functional optical applications, this has imposed great challenges in the design and precision machining. In this paper, the improved grinding technology was evaluated by two methods: sample optical measure and specific freeform surface manufacturing. In the design of freeform optics, there were emerging methodologies for the mathematical description of freeform optics [14,15]. In this study, the mother mirror of the experimental sample was biconic Zernike freeform surface, and its expression was:

$$z = \frac{c_x x^2 + c_y y^2}{1 + \sqrt{1 - (1 + k_x)c_x^2 x^2 - (1 + k_y)c_y^2 y^2}} + \sum_{i=1}^{16} \alpha_i x^i + \sum_{i=1}^{16} \beta_i y^i + \sum_{i=1}^{N} A_i Z_i(\rho, \varphi) \quad (1)$$

Equation (1) included four parts. The first part was the basic term of the hyperbolic quadric surface of the whole surface, the second and third parts were the high-order aspherical terms in X and Y directions respectively, and the fourth part was the Zernike term. In the formula, $c_x = 1/255.98$ and $c_y = 1/253.38$ were the curvatures in the X and Y directions respectively, $k_x = -0.977$ and $k_y = -0.978$ were conic coefficients in X and Y directions respectively, $\alpha_i = 0$ and $\beta_i = 0$ were high-order aspheric coefficients in X and Y directions respectively, A_i were Zernike polynomial coefficients, $A_1 = -4.537$, $A_2 = 4.609 \times 10^{-4}$, $A_3 = 0.114$, $A_4 = -0.205$, $A_5 = -4.828 \times 10^{-5}$, $A_6 = 0.0679$, $A_7 = 6.743 \times 10^{-3}$, $A_8 = 1.191 \times 10^{-5}$, $A_9 = -2.872 \times 10^{-5}$. Z_i (ρ,θ) were the standard Zernike polynomials, the normalized radius was 130 mm.

According to the improved grinding technology, the grinding was carried out based on the same grinding equipment of the Section 2.1. The freeform surface was analyzed based on the optical design file by coordinate transformation, and the point cloud coordinates of the freeform surface were input into the machine. The grinding process was divided into two stages: rough grinding and fine grinding. The processing parameters are shown in Table 2.

Table 2. Processing parameters in grinding.

	Parameters	Rough Grinding	Fine Grinding
1	Cut speed	20 m/s	20 m/s
2	Remove depth	0.1 mm	0.01 mm
3	Diamond size	91 μm	18 μm
4	Feed speed	200 mm/min	200 mm/min
5	Path	spiral	spiral

Bonnet polishing is a relatively mature small head processing method at present. Generally, a spherical flexible body made of rubber with appropriate hardness was used as the support of the polishing pad. With the adjustment of different air pressure, different removal functions can be obtained, which can effectively adapt to the deterministic processing under different surface input conditions [16]. In addition, the bonnet polishing head was a convex spherical surface with small curvature, which can achieve a good fit between the bonnet polishing head and the workpiece contact area. Based on the high-precision and multi degree of freedom kinematic mechanism, it can complete the processing of various large deviations freeform surfaces. Polyurethane, polishing cloth, pitch, and other materials can be selected for the bonnet polishing pad. In general, polyurethane and polishing cloth can be used to correct the low frequency surface shape, pitch can be used to improve the middle and high frequency surface shape, and high-precision convergence in full frequency band can be achieved through a combined process.

In this paper, polishing was performed on the Optotech MCP-251 (Optotech, Wettenberg, Germany) using cerium oxide slurry (Cerrox 1663, Lille, France) set at Baume 4

and pH 9, which was recirculated through a filtration system. The processing parameters, which were verified and showed in Table 3, can be selected in different processing stages.

Table 3. Processing parameters in bonnet polishing.

No.	Parameters	Pre Polishing	Smoothing	Precision Polishing
1	Speed	651 rpm	100 rpm	751 rpm
2	Path	raster	spiral	raster
3	Spot size	10 mm	10 mm	5 mm
4	Polishing pad	polyurethane	pitch	cloth
5	Pressure	1.0 bar	0.1 bar	1.0 bar

2.4. Process Flow of Verification

The improved grinding technology can reduce the SSD, and further reduce the total removal amount of polishing as well as the mid-frequency residue of polishing track. In the grinding stage, the grinding surface with low SSD was obtained by the improved grinding technology and measured by the CMM. In the polishing stage, removing surface damage and correcting surface shape error were two important objectives. The power spectral density (PSD) can evaluate the surface shape error of the whole frequency band on the basis of the processing results, and further indirectly validated the grinding effect. The surface shape error was dominated by low frequency at the initial stage of surface error correction, so that the tool with corresponding dimensions can be used. In the middle state of processing, the surface shape error was mainly the mid frequency, and the size of the tool should be reduced with the reduction in the error period, but usually the size should be greater than 5 mm. At the later stage of processing, the surface shape error was mainly by medium and high frequencies. It was necessary to change the error cycle through the smoothing effect of large-scale tools. The process flow diagram is shown in Figure 3.

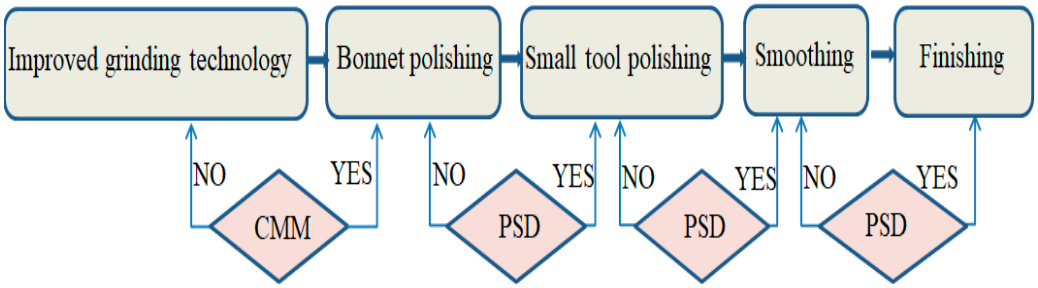

Figure 3. Process flow of combined processing.

3. Results

3.1. Results of the Improved Grinding Technology

According to the experimental design listed in Table 1 and test analysis methods above, the paper analyzes eight groups of experimental data. Firstly, the effect of removal depth on subsurface damage was investigated. Figure 4 shows example microscope images at fixed depths of 3, 6, 10, and 14 μm along the polished wedge of the ground surfaces for each of the sample parts. The abscissa represents the depth corresponding to the detection position, and the ordinate represents the different grinding removal depths in the process parameters. The character of the individual microcracks was similar to the sample part, as observed in previous studies [9], the depth was determined by the profilometer, and the damage characteristics of SSD can be easily visually compared in Figure 4 by ranking the degree of crackle at a fixed depth.

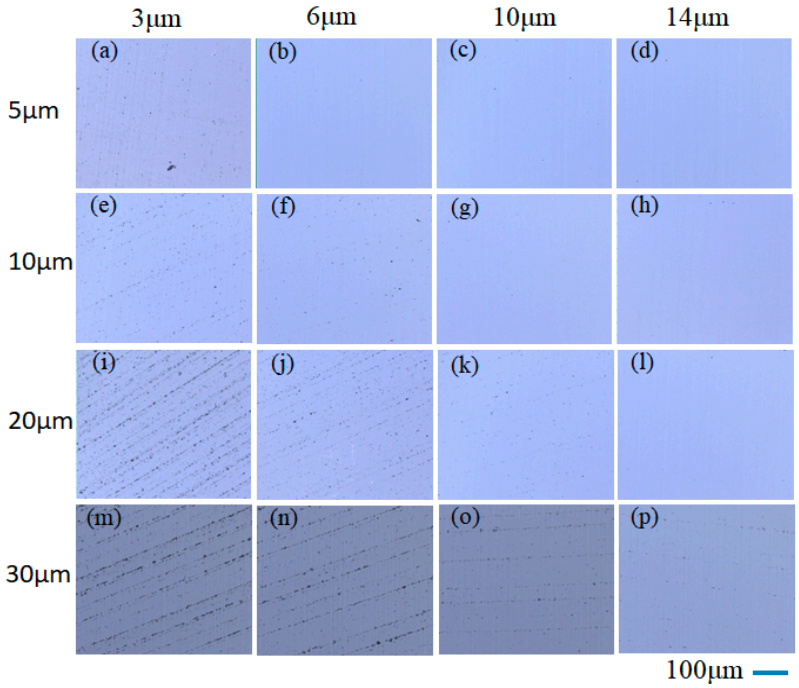

Figure 4. Optical micrographs of the SSD fractures observed after polishing to the depths of 3, 6, 10, and 14 μm under different grinding removal depths. Polishing (**a**) 3 μm, (**b**) 6 μm, (**c**) 10 μm, (**d**) 14 μm when grinding 5 μm. Polishing (**e**) 3 μm, (**f**) 6 μm, (**g**) 10 μm, (**h**) 14 μm when grinding 10 μm. Polishing (**i**) 3 μm, (**j**) 6 μm, (**k**) 10 μm, (**l**) 14 μm when grinding 20 μm. Polishing (**m**) 3 μm, (**n**) 6 μm, (**o**) 10 μm, (**p**) 14 μm when grinding 30 μm.

According to the surface morphology shown in Figure 4b,g,l, there were no damage features. It was believed that the depth at this location was the SSD depth. The relationship between removal depth and SSD depth was summarized in Figure 5. The curve showed that with the continuous increase in removal depth, the SSD increased gradually. It should be pointed out that this was the average of three measurements at different positions of the workpiece.

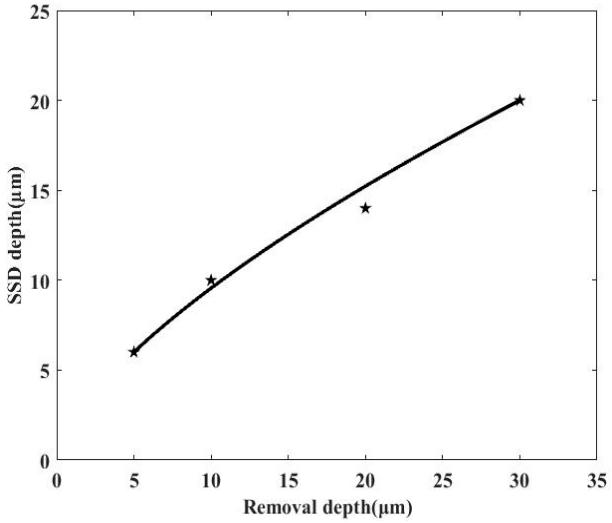

Figure 5. The relationship between removal depth and SSD depth.

The effect of cutting speed on SSD is shown in Figure 6. The abscissa represents microscope images at fixed depths of 3, 6, 10, and 14 μm along with the polished wedge

of the ground surfaces for each of the sample parts. The ordinate represents microscope images at a fixed speed 12 m/s, 18 m/s, 24 m/s, 30 m/s.

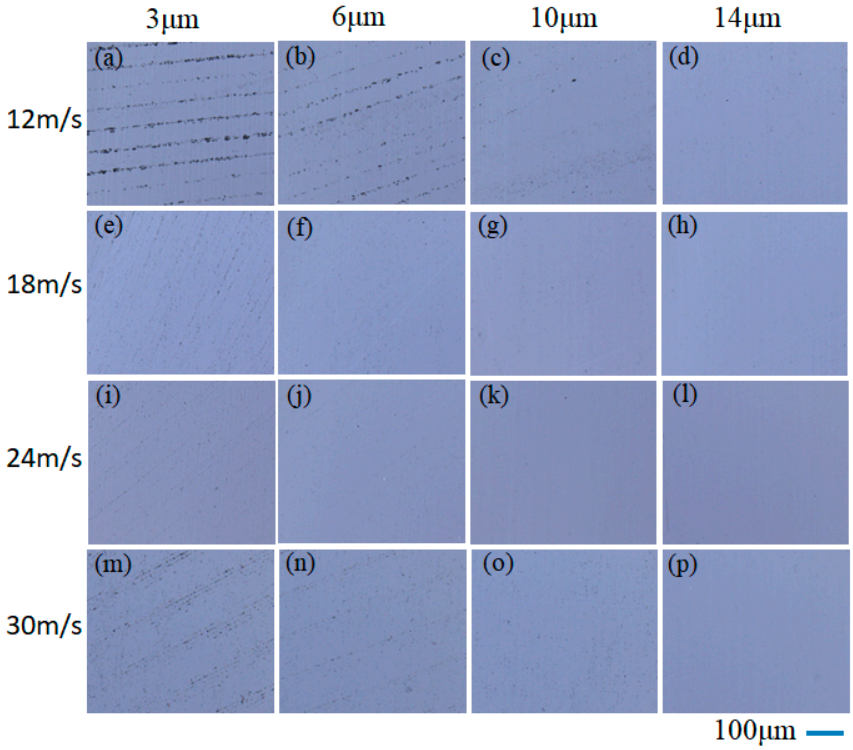

Figure 6. Optical micrographs of the SSD fractures observed after polishing to the depths of 3, 6, 10, and 14 μm under different cutting speeds. Polishing (**a**) 3 μm, (**b**) 6 μm, (**c**) 10 μm, (**d**) 14 μm when cutting speed 12 m/s. Polishing (**e**) 3 μm, (**f**) 6 μm, (**g**) 10 μm, (**h**) 14 μm when cutting speed 18 m/s. Polishing (**i**) 3 μm, (**j**) 6 μm, (**k**) 10 μm, (**l**) 14 μm when cutting speed 24 m/s. Polishing (**m**) 3 μm, (**n**) 6 μm, (**o**) 10 μm, (**p**) 14 μm when cutting speed 30 m/s.

Figure 6 shows that there was no damage feature in (d,g,k,p). It was believed that the depth at this location was the SSD depth. This paper summarized the depth corresponding to the disappearance of damage characteristics at different cutting speeds. It should be emphasized that the depths here were the average of three different slopes. It can be seen from Figure 7 that with the continuous increase in cutting speed, the SSD increased gradually in a certain range, when exceeding a certain range, the SSD tended to increase.

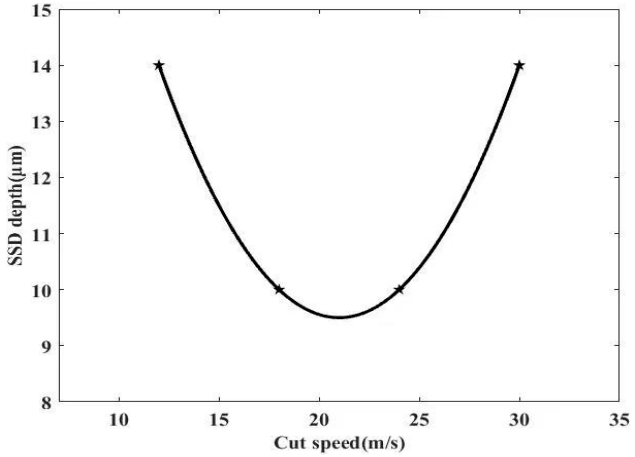

Figure 7. The relationship between cutting speed and SSD depth.

3.2. Results of the Experimental Verification on Freeform

In this paper, a general grinding technology was developed and then applied to freeform machining. The improved grinding technology had a good application performance in hard and brittle materials grinding, and its effect has been further confirmed through precision polishing. The grinding processing and result were carried out based on the same grinding equipment of the Section 2.1 (as shown in Figure 8).

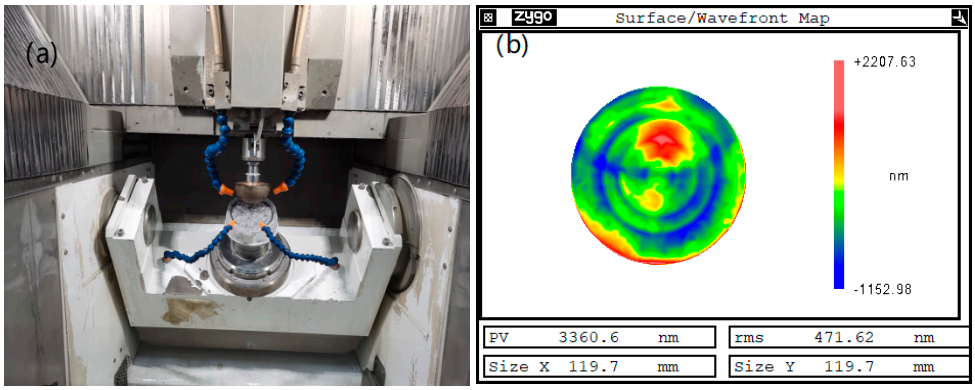

Figure 8. Grinding process and results, (**a**) Grinding, (**b**) final surface figure.

In this study, bonnet polishing was applied to the precision polishing of freeform surfaces to evaluate the application effect of the improved grinding technology. In this process, the polishing removal depth was obtained by the thickness change in the element, and the surface characteristics were confirmed by the optical microscope. The final results show that when the removal depth was 10 μm, the surface has no damage, and the surface shape error reaches 12.1 nm rms. The polishing processing and result areshown in Figure 9.

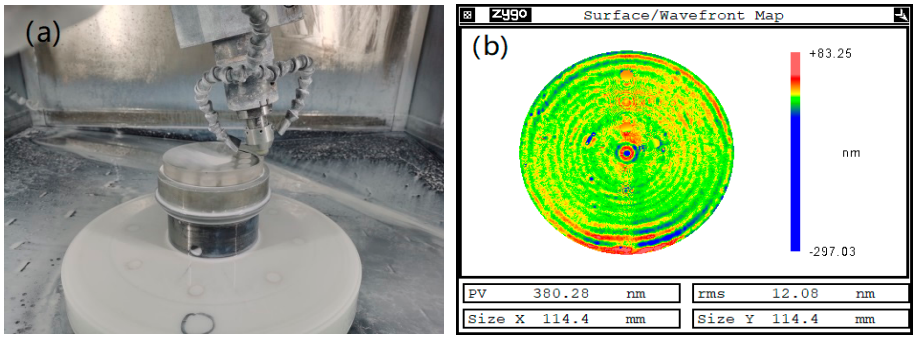

Figure 9. Bonnet polishing process and result, (**a**) Bonnet polishing, (**b**) final surface figure.

4. Discussion

Generally, the complexity of the grinding process had historically made it challenging to predict SSD depth distributions and surface shape error for various grinding parameters and different materials. Plastic removal in the processing of hard and brittle materials was an effective way to reduce SSD [17]. The orthogonal experiment of sample grinding showed the preliminary rule. Reducing the amount of material removal brings the removal process infinitely close to plastic removal, and reduces the SSD, which was consistent with our experimental results. In a certain range, increasing the cutting speed of the grinding tool can improve the material removal effect, reduce the removal stress between the grinding tool and the material, and further improve the surface quality. There were several error sources in this experiment. One was the sampling and judgment of damage features, another was the location determination of damage features. In addition, the limited number of samples was also a factor affecting the measurement accuracy, but this did not affect its application.

Considering the above factors, the measurement accuracy of the experiments was better than 2 μm.

In addition, the machining parameters also had a great impact on the vibration of the machine, which will affect the mid-frequency of the ground surface. The mid-frequency usually appeared as rings on the surface, and it will take a lot of time to remove them in polishing. Therefore, optimizing the cutting speed and removal depth were very important, in order to reduce the SSD and improve the surface quality of components, as demonstrated by experiments and analyses in this paper. The above conclusions will be further verified in the subsequent freeform surface machining, and applied as a general technology to the machining of hard and brittle materials.

It was difficult to measure the surface shape error of the grinding surface in full frequency band, because the surface roughness at this stage cannot meet the requirements of optical measurement. However, it was an effective method to indirectly evaluate the grinding quality through the measurement results after polishing. In the specific freeform surface manufacturing verification, the depth of the SSD obtained by the change in the thickness has a good correspondence with the previous experimental results. The resolution of the optical interferometer can be better than 0.3 mm, which was very important for the evaluation of the polished surface characteristics. Figure 10 shows the comparative effect of traditional grinding and improved grinding after removing 1 μm by bonnet polishing. The values of mid-frequency with 2–10 mm band pass were provided to show the improvement effect. It can be seen from the figure that the value of mid-frequency was reduced from 40.9 nm to 24.8 nm rms, and the improvement effect was very obvious.

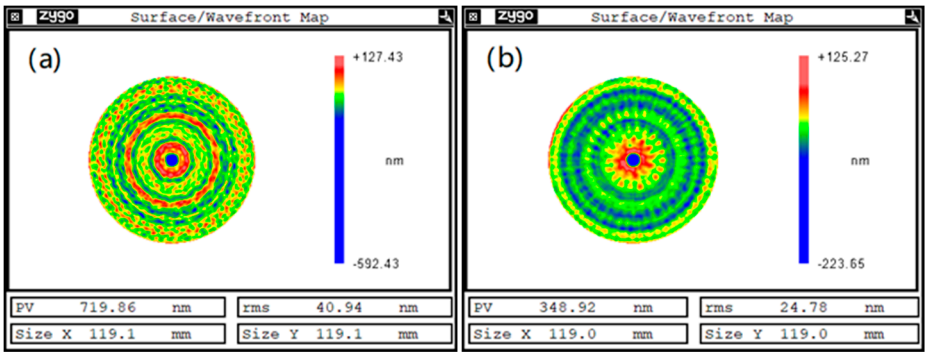

Figure 10. Mid-frequency with 2–10 mm band pass. (**a**) Traditional grinding, (**b**) Improved grinding.

The technology objective of improved grinding technology was to reduce the SSD and the full-frequency surface shape error of the ground surface, and further improve the convergence efficiency of polishing. Figure 11 shows the typical machining results of three rounds in the machining process. The paper analyzed the full band convergence efficiency in the process of bonnet polishing, and found that the convergence rate was about 30% to 50%. There was a relatively stable convergence rate in bonnet polishing, which indicated that the surface shape error of the ground surface was mainly low frequency.

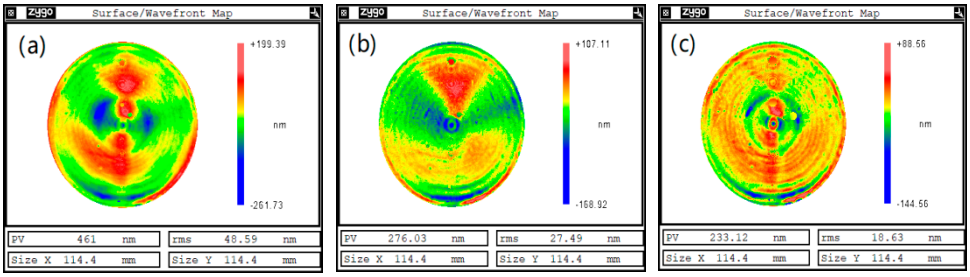

Figure 11. Bonnet polishing typical surface figure, (**a**) run 1, (**b**) run 2, (**c**) run 3.

In order to evaluate the impact of polishing processing on various frequency bands more accurately, the results of three rounds of processing in the process were analyzed by PSD, as shown in Figure 12. It can be seen from the figure that the PSD curve decreases steadily, but the error convergence rate of different periods was slightly different. It was necessary to further adjust and optimize the polishing tool design and processing parameters to achieve convergence of the surface error stable.

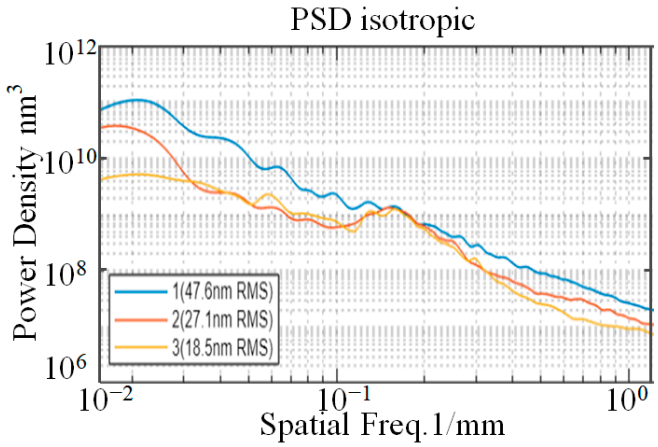

Figure 12. PSD curve comparison of three rounds results in full frequency band.

5. Conclusions

In this paper, an improved grinding technology was developed for manufacturing of optical freeform surfaces, which was characterized by low SSD and high surface quality. More importantly, this general technology has been fully verified in the manufacture of freeform. The specific conclusions can be summarized as follows:

(1) The influence of key process factors such as cutting speed and removal depth during the grinding process was obtained through orthogonal experiments. The results showed that when the cutting speed was about 20 m/s and the removal depth was 10 μm, the SSD was reduced from 20 μm to 10 μm and the surface shape accuracy (PV) was better than 5 μm.

(2) We applied the improved grinding technology to the machining of freeform surfaces and completed the engineering verification of the process. Compared with traditional grinding, the value of mid-frequency with 2–10 mm band pass was reduced from 40.9 nm to 24.8 nm rms, and the final surface figure was better than 12.1 nm rms. The manufacturing accuracy and efficiency had been significantly improved, which supported the developing of intelligent extreme manufacturing.

The grinding technology and evaluation method studied in this paper improved the application level of traditional grinding technology in the manufacturing of hard and brittle materials. However, the SSD test method based on MRF was a destructive measurement method, which can only be used for sample components. Besides, the indirect evaluation of the ground surface by polishing was lacked timeliness. In the future, higher level ultra-precision grinding technology, higher resolution contact, and non-contact testing technology of the ground surface will be the focus of further research.

Author Contributions: Conceptualization and methodology, X.Z. (Xiaoqin Zhou) and X.Z. (Xuejun Zhang); optical measurement, Q.C. and L.L.; Experiment and verification, L.P. and X.L. (Xingchang Li); writing—manuscript and editing, L.P.; Project administration, X.L. (Xiao Luo); All authors have read and agreed to the published version of the manuscript.

Funding: The work was funded by the National Natural Science Foundation of China (62127901, 12203048, 12003034, 61975201).

Institutional Review Board Statement: Not applicable.

Informed Consent Statement: Not applicable.

Data Availability Statement: Data are contained within the article.

Conflicts of Interest: The authors declare no conflict of interest.

References

1. Zhu, W.-L.; Beaucamp, A. Compliant grinding and polishing: A review. *Int. J. Mach. Tools Manuf.* **2020**, *158*, 103634. [CrossRef]
2. Yu, G.; Walker, D.D.; Li, H. Research on fabrication of mirror segments for E-ELT. In Proceedings of the 6th International Symposium on Advanced Optical Manufacturing and Testing Technologies: Advanced Optical Manufacturing Technologies, Xiamen, China, 26–29 April 2012; Volume 8416, p. 841602. [CrossRef]
3. Xiong, L.; Qi, E.; Luo, X.; Zhang, F.; Xue, D.; Zhang, X. Stitching swing arm profilometer test for large aperture aspherics. *Chin. Opt. Lett.* **2019**, *17*, 112201. [CrossRef]
4. Lin, B.; Li, S.-P.; Cao, Z.-C.; Zhang, Y.; Jiang, X.-M. Theoretical modeling and experimental analysis of single-grain scratching mechanism of fused quartz glass. *J. Mater. Process. Technol.* **2021**, *293*, 117090. [CrossRef]
5. Xiao, H.; Wang, H.; Yu, N.; Liang, R.; Tong, Z.; Chen, Z.; Wang, J. Evaluation of fixed abrasive diamond wire sawing induced subsurface damage of solar silicon wafers. *J. Mater. Process. Technol.* **2019**, *273*, 116267. [CrossRef]
6. Zhang, Z.; Yan, J.; Kuriyagawa, T. Manufacturing technologies toward extreme precision. *Int. J. Extreme Manuf.* **2019**, *1*, 022001. [CrossRef]
7. Chen, S.; Yang, S.; Liao, Z.; Cheung, C.F.; Jiang, Z.; Zhang, F. Curvature effect on surface topography and uniform scallop height control in normal grinding of optical curved surface considering wheel vibration. *Opt. Express* **2021**, *29*, 8041–8063. [CrossRef]
8. Xiao, H.; Yin, S.; Wu, H.; Wang, H.; Liang, R. Theoretical model and digital extraction of subsurface damage in ground fused silica. *Opt. Express* **2022**, *30*, 17999–18017. [CrossRef]
9. Suratwala, T.I.; Steele, W.A.; Wong, L.A.; Tham, G.C.; Destino, J.; Miller, P.E.; Ray, N.; Menapace, J.A.; Feigenbaum, E.; Shen, N.; et al. Subsurface mechanical damage correlations after grinding of various optical materials. *Opt. Eng.* **2019**, *58*, 092604. [CrossRef]
10. Dong, Z.; Cheng, H. Developing a trend prediction model of subsurface damage for fixed-abrasive grinding of optics by cup wheels. *Appl. Opt.* **2016**, *55*, 9305–9313. [CrossRef]
11. Suratwala, T.; Menapace, J.; Tham, G.; Steele, W.; Wong, L.; Ray, N.; Bauman, B. Understanding and reducing mid-spatial frequency ripples during hemispherical sub-aperture tool glass polishing. *Appl. Opt.* **2022**, *61*, 3084. [CrossRef]
12. Lambropoulos, J.C.; Xu, S.; Fang, T. Loose abrasive lapping hardness of optical glasses and its interpretation. *Appl. Opt.* **1997**, *36*, 1501–1516. [CrossRef]
13. Lin, B.; Jiang, X.-M.; Cao, Z.-C.; Huang, T.; Li, K.-L. Theoretical and experimental analysis of material removal and surface generation in novel fixed abrasive lapping of optical surface. *J. Mater. Process. Technol.* **2020**, *279*, 116570. [CrossRef]
14. Falaggis, K.; Rolland, J.; Duerr, F.; Sohn, A. Freeform optics: Introduction. *Opt. Express* **2022**, *30*, 6450–6455. [CrossRef]
15. Shi, Y.; Zheng, Y.; Lin, C.; Ji, Z.; Zhang, J.; Han, Y.; Tian, L.; Hu, D. Design Method of Freeform Anamorphic Telescopes with an Ultrawide Field of View. *Photonics* **2022**, *9*, 836. [CrossRef]
16. Su, X.; Ji, P.; Liu, K.; Walker, D.; Yu, G.; Li, H.; Li, D.; Wang, B. Combined processing chain for freeform optics based on atmospheric pressure plasma processing and bonnet polishing. *Opt. Express* **2019**, *27*, 17979–17992. [CrossRef]
17. Chen, S.; Yang, S.; Liao, Z.; Cheung, C.F.; Jiang, Z.; Zhang, F. Study of deterministic surface micro-texture generation in ultra-precision grinding considering wheel oscillation. *Opt. Express* **2022**, *30*, 5329. [CrossRef]